DOI 10.1007/s10778-017-0807-5
International Applied Mechanics, Vol. 53, No. 2, March, 2017

INFLUENCE OF ELECTRIC LOADING CONDITIONS ON THE VIBRATIONS OF PIEZOCERAMIC RESONATORS

V. L. Karlash

Experimental data for the fundamental radial mode of a thin piezoceramic disk are analyzed. It is established that the voltage drops and instantaneous powers are very sensitive to the loading conditions, while admittances, impedances, and phase shifts do not depend on them. If the current is set constant, the instantaneous power decreases as the resonance is approached and increases as the antiresonance is approached. If the voltage is set constant, the instantaneous power increases as the resonance is approached and decreases as the antiresonance is approached

Keywords: piezoceramic resonator, instantaneous power, admittance, impedance, phase shift, efficiency

Introduction. The vibrations of structural members made of piezoceramics are distinguished by strong coupling of strains and electric-field strength [1–4, 8–11, 17]. Experimental studies usually involve direct or indirect measurements of resonant/antiresonant frequencies and associated admittances and impedances. A piezoresonator of interest is connected in series with a pull-up resistor or a capacitor, and the voltage drop across it and its load are used to calculate the admittances and impedances. To calculate the amplitudes of mechanical displacements, strains, and stresses as well as the amplitudes of admittances and powers, it is necessary to take into account energy losses [2, 8–11, 25–27], which are currently considered to have mechanical, dielectric, and piezoelectric components [10, 11, 19–22, 25–27].

In [1, 2, 8, 11, 24] it was shown that the behavior of piezoresonators strongly depends on the electric loading conditions and differs in the cases of set (constant-amplitude) current and set (constant-amplitude) voltage drop. In experiments on the longitudinal vibrations of rectangular piezoceramic plates in [25–27], it was found out that the admittance–frequency response at voltage of constant amplitude is essentially nonlinear, including abrupt drops and jumps. Such nonlinearity is absent if the current is of constant amplitude. It was also shown that the current cannot be maintained constant at the antiresonance if the power is high. It was proposed to determine the resonant and antiresonant characteristics of high-power piezoresonators at current of constant amplitude and voltage of constant amplitude, respectively.

Here we will analyze experimental data in the frequency range near the first radial mode of a thin piezoceramic disk in an advanced Mason circuit [8, 12, 13, 18, 24] and its *R*-, *C*-, and *L*-models. The input voltage U_{in} and the voltage drops across the piezoelectric element, U_{pe}, and the pull-up resistor, U_R, measured "as is" were reduced to the cases where current, voltage drop, input power, or piezoelement power is set constant.

It was established that the voltage drops, input power, and piezoelement power strongly depend on the loading conditions, whereas the admittance, impedance, and phase shifts between the components of admittance do not depend on them. If the current is set constant, the instantaneous power decreases as the resonance is approached and increases as the antiresonance is approached. If the voltage is set constant, the instantaneous power increases as the resonance is approached and decreases as the antiresonance is approached.

S. P. Timoshenko Institute of Mechanics, National Academy of Sciences of Ukraine, 3 Nesterova St., Kyiv, Ukraine 03057, e-mail: karlashv@ukr.net. Translated from Prikladnaya Mekhanika, Vol. 53, No. 2, pp. 124–134, March–April, 2017. Original article submitted June 11, 2015.

1. Experimental Procedure. Treatment of the Experimental Data. A noticeable difference between the constant-current and constant-voltage modes is observed in high-power ultrasonic devices such as radiators, motors, or transformers.

According to [27], there are severe difficulties in determining the electromechanical-coupling parameters under high electric loads at constant voltage because of the strong nonlinearity of the admittance–frequency response at resonances, including drops and jumps. If the current amplitude is set constant, then, though nonlinearity is not observed at resonance, this mode cannot be provided at antiresonance when power is high.

With the classical Mason two-port network, it is difficult to provide constant-current or constant-voltage modes [3, 4, 11, 16]. The improvements proposed in [12, 13, 18, 24] considerably facilitate the measurement of amplitudes and increase their accuracy. To eliminate the effect of the measuring circuit on the ultrasonic generator, a matching resistance divider is connected between them [3, 4, 16]. The measuring circuit consisting of a piezoelectric element of P_e and a pull-up resistor R_p connected in series is connected in parallel to the output resistor of the matching divider and shunts it to some extent. The shunting effect of the measuring circuit is especially noticeable at and near resonances. If the set voltage is maintained at the output of the generator, then three voltage drops simultaneously change during frequency tuning: the input voltage U_{in} of the measuring circuit, the voltage drop Upe across the piezoelectric element, and the voltage drop U_R across the pull-up resistor. This is the "as is" loading conditions. If the amplitude of one of the voltages U_{in}, U_{pe}, and U_R is maintained constant, then either voltage or current is set. Data from such experiments are reported in [1, 2, 8, 20] where it is shown that near the resonant frequencies, only the voltages U_{in}, U_{pe}, and U_R change, whereas the admittances and phase shifts between voltage drops remain the same. The same result was obtained in modeling a piezoresonator by passive *R*-, *C*-, and *L*-elements [20, 21]. The author's experience suggests that labor-intensive multiple measurements in various electric loading conditions can be simplified if we take into account the fact that for weak electric fields (approximately 1 V/mm at resonances), a piezoceramic materials remain linear. The quantities U_{in}, U_{pe}, and U_R (and the respective frequencies) measured "as is" with an advanced Mason circuit at different frequencies are entered into a computer to plot the frequency responses for voltage drops, admittances, impedances, phase shifts, instantaneous powers, etc. The admittance is calculated by the following exact formula [20, 21]:

$$Y_{pe} = \frac{I_{pe}}{U_{pe}} = \frac{U_R}{RU_{pe}} \tag{1}$$

or by the two approximate formulas

$$Y_{pe1} = \frac{U_R}{R(U_{in} - U_R)}, \tag{2}$$

$$Y_{pe2} = \frac{(U_{in} - U_{pe})}{RU_{pe}}. \tag{3}$$

All the three formulas yield identical results at resonant and antiresonant frequencies. At frequencies far from these resonances, the results differ substantially.

The phase shifts are determined using the cosine theorem [1, 2, 13, 24]:

$$\cos\alpha = \frac{U_{pe}^2 + U_R^2 - U_{in}^2}{2U_{pe}U_R}, \quad \cos\beta = \frac{U_{in}^2 + U_R^2 - U_{pe}^2}{2U_{in}U_R}, \quad \cos\gamma = \frac{U_{in}^2 + U_{pe}^2 - U_R^2}{2U_{in}U_{pe}}. \tag{4}$$

The instantaneous power is the product of the current in the piezoelectric element and the voltage drop across it:

$$P_{pe} = U_{pe}I_{pe} = \frac{U_R U_{pe}}{R}, \quad P_{in} = U_{in}I_{pe} = \frac{U_R U_{in}}{R}, \quad P_R = U_R I_{pe} = \frac{U_R U_R}{R}, \tag{5}$$

where P_{in} is the instantaneous input power; P_{pe} is the instantaneous power for the specimen; P_R is the instantaneous power across the pull-up resistor.

The "as is" loading conditions can be transformed to other conditions (when amplitudes are low) as follows:

$$U_{\text{in}} = U_{\text{in}\,00}, \quad U_{\text{pe}} = U_{\text{in}\,00}U_{\text{pe}0}/U_{\text{in}\,0}, \quad U_R = U_{\text{in}\,00}U_{R0}/U_{\text{in}\,0}, \quad U_R = U_{R00},$$

$$U_{\text{in}} = U_{R00}U_{\text{in}\,0}/U_{R0}, \quad U_{\text{pe}} = U_{R00}U_{\text{pe}0}/U_{R0}, \quad U_{\text{pe}} = U_{\text{pe}00}, \quad U_{\text{in}} = U_{\text{pe}00}U_{\text{in}\,0}/U_{\text{pe}0},$$

$$U_R = U_{\text{pe}00}U_{R0}/U_{\text{pe}0}, \quad p_0 = p_{00}, \quad t = [p_0/(U_{R0}U_{\text{pe}0})]^{1/2}, \quad U_{\text{pe}} = U_{\text{pe}0}t,$$

$$U_R = U_{R0}t, \quad U_{\text{in}} = U_{\text{in}\,0}t, \quad p_{\text{in}\,0} = p_{\text{in}\,00}, \quad t_{\text{in}} = [p_{\text{in}\,0}/(U_{R0}U_{\text{pe}0})]^{1/2},$$

$$U_{\text{pe}} = U_{\text{pe}0}t_{\text{in}}, \quad U_R = U_{R0}t_{\text{in}}, \quad U_{\text{in}} = U_{\text{in}\,0}t_{\text{in}}, \tag{6}$$

where $U_{\text{in}\,00}, U_{\text{pe}00}, U_{R00}, p_{00}$, and $p_{\text{in}\,00}$ are set amplitudes; $U_{\text{in}\,0}, U_{\text{pe}0}, U_{R0}$ are measured "as is."

The frequency responses of voltage drops plotted by formulas (6) indicate what values of U_{in}, U_{pe}, and U_R at some frequencies should be to provide the set electric loading conditions. The frequency responses for admittance, phase shifts, and instantaneous power allow evaluating the effect of various factors on the characteristics of oscillations of piezoresonators.

Measurements were made on a thin TsTBS-3 piezoceramic disk 66.4 mm in diameter and 3.1 mm in thickness. First, an E8-12 alternating-current bridge was used to measure the interelectrode capacitance and dielectric losses. Then the characteristic frequencies and admittances were measured with an advanced Mason circuit, and amplitude- and phase–frequency response were plotted. The frequency of a G3-56/1 generator with an input resistance of 50 Ω was controlled with a Ch3-38 digital frequency meter. The voltage drops were measured by a V3-38 millivoltmeter or a V2-27A/1 digital multimeter. The matching divider consisted of two resistors 68 and 10 Ω.

The disk had static self-capacitance $C_0 = 18.5$ nF, dielectric loss tangent $e_{33m} = 0.0085$, mechanical loss tangent $s_{11m} = 0.0069$, Poisson's ratio $n = 0.35$, planar EMCC $k_{po}^2 = 0.31$, and piezoelectric loss tangent $d_{31m} = 0.0076$. The pull-up resistor was 11.2 Ω near the resonance and 20.1 Ω near the antiresonance. It was found out that the frequency of maximum admittance $f_m = 31.551$ kHz, maximum admittance $Y_m = 127.1$ mS, conductivity at –3dB $Y_{-3\text{db}} = 89.87 \cong 90$ mS, difference of pass-band limits $f_2 - f_1 = 22/28 \times 300 = 235.7$ Hz, Q-factor at resonance $Q_r = 31551/235.7 = 138.8$; frequency of maximum impedance $f_n = 36{,}499$ kHz, maximum impedance $Z_n = 16.86$ kΩ, impedance at –3dB $Z_{-3\text{db}} = 11.92$ kΩ, difference of pass-band limits $f_2 - f_1 = 31/33 \times 200 = 187.7$ Hz, Q-factor at antiresonance $Q_a = 36499/187.9 = 194.2$.

The oscillating system of a piezoelectric resonator can be represented [8, 20, 21] as an electrical circuit in which the static interelectrode capacitance C_0 is connected in parallel to series-connected inductor *L*, capacitor *C*, and resistor *r*, which represents energy losses. In radio engineering, such a system is called a circuit of the third kind [6]. The resonance of voltages in the *L–C–r* circuit corresponds to the resonant frequency at which $r = 1/Y_m$. The resonance of currents in the parallel circuit corresponds to the antiresonant frequency. This circuit consists of the same inductor *L* and equivalent capacitor C' formed by series-connected capacitors C_0 and C ($C' = C_0C/(C_0 + C)$).

In radio engineering, the Q-factor of a resonant system is determined as the ratio of the energy E_{stor} stored in the circuit to the energy $E_{\text{dis.av}}$ dissipated over a period of oscillations. It is expressed in terms of the parameters of the circuit as follows [5, 6]:

$$Q = 2\pi\frac{E_{\text{stor}}}{E_{\text{dis.av}}} = \frac{\rho}{r} = \frac{2\pi f_0 L}{r} = \frac{1}{2\pi f_0 Cr}, \quad \rho = \sqrt{\frac{L}{C}}, \quad f_0 = \frac{1}{2\pi\sqrt{LC}}, \tag{7}$$

where ρ is the wave impedance; *r* is the loss resistor; f_0 is the resonant frequency; *L* and *C* are the inductance and capacitance of the circuit.

The equivalent capacitance and inductance can be calculated by the following simple formulas:

$$C = \frac{1}{\rho\omega} = \frac{1}{2\pi f_0\rho} = \frac{1}{2\pi f_0 Q_r r}, \quad L = \frac{\rho}{\omega} = \frac{\rho}{2\pi f_0} = \frac{Q_r r}{2\pi f_0}. \tag{8}$$

The parameters of the 66.4×3.1 mm disk with a pull-up resistor of 11.2 Ω are the following: $r = 7.87$ Ω, $Q_r = 138.8$, and $\rho = Q_r \cdot r = 1092$ Ω, $f_0 = 3.155 \cdot 10^4$ Hz, $C_0 = 1.849 \cdot 10^{-8}$ F. Substituting these values into formula (8), we obtain

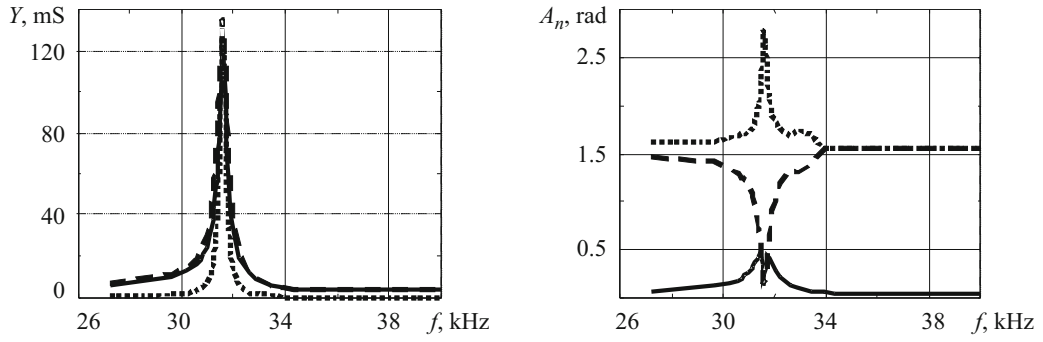

Fig. 1

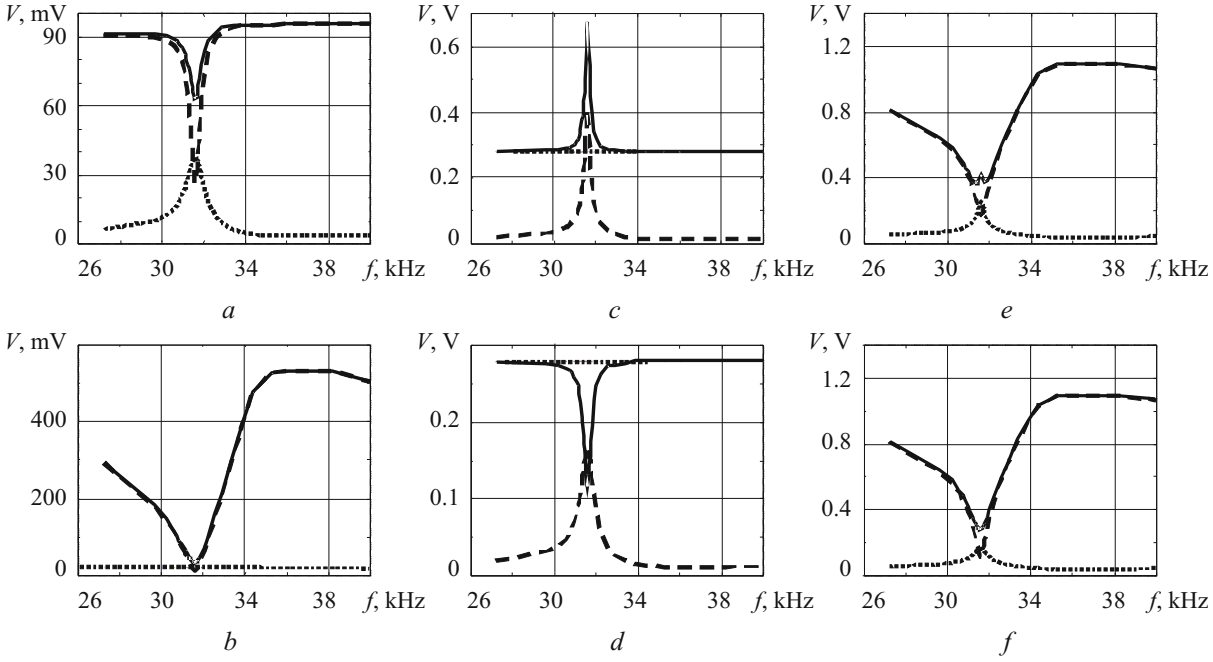

Fig. 2

$C = 1/(2\cdot 3.14\cdot 1.092\cdot 3.155\cdot 10^7)\,\text{F} = 1/(2.164\cdot 10^8)\,\text{F} = 4.62\cdot 10^{-9}$ F, $L = 1092/(2\cdot 3.14\cdot 3.155\cdot 10^4)\,\text{Hz} = 5.51\cdot 10^{-3}$ H. The capacitance of the parallel circuit $C' = C\cdot C_0/(C + C_0) = 4.62\cdot 18.49/(4.62 + 18.49)\cdot 10^{-9}$ F = $3.696\cdot 10^{-9}$ F.

The parallel resonance (antiresonance) frequency, wave impedance, and Q-factor at antiresonance are as follows: $f_n = 3.528\cdot 10^4$ Hz, $\rho = 1221\,\Omega$, $Q_a = 1221/7.87 = 155.1$.

In modeling the disk by an equivalent circuit consisting of passive elements $L = 4$ mH, $C = 6.719$ nF, and $C_0 = 25.22$ nF, the frequency of maximum conductivity $f_m = 30{,}805$ kHz, maximum admittance $Y_m = 95.6$ mS, the frequency of maximum impedance $f_n = 34{,}734$ kHz, maximum impedance $Z_n = 2.6$ kΩ. These parameters are close to the parameters of the real disk, except for the maximum impedance. The difference may be due to the shunting effect of the output resistor of the matching divider.

2. Influence of the Electric Loading Conditions on the Characteristics of Oscillations of the Piezoceramic Disk. Figure 1 shows the admittance–frequency responses (Fig. 1*a*) plotted by formulas (1)–(3) (solid, dotted, and dashed curves, respectively) and phase shifts (Fig. 1*b*) as arccosines of formulas (4). Neither conductivity, nor angles depend on the loading conditions and are presented here as an example. The angle α (dashed line) is formed by the sides U_{pe} and U_R of the triangle. It characterizes the phase shift between the current through and the voltage drop across the piezoelectric element. The angle β (discontinuous curves) is formed by the sides U_{in} and U_R and characterizes the phase shift between the output voltage and the

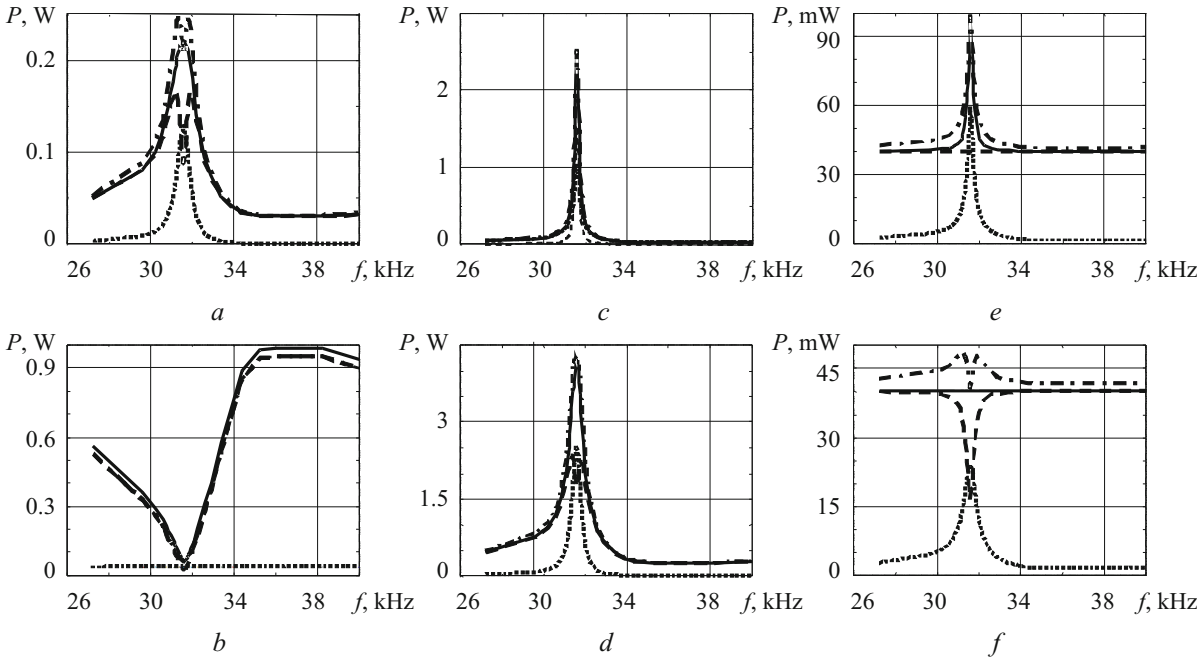

Fig. 3

consumed current. The angle γ (solid lines) is formed by the sides U_{in} and U_{pe}, i.e., it is the phase shift between the output voltage of the generator and the voltage drop across the piezoelectric element.

When the "as is" conditions are changed to other electric loading conditions using formulas (6), the frequency responses of voltage drops (Fig. 2) and instantaneous powers (Fig. 3) change considerably. The curves represent the "as is" conditions (Fig. 3*a*), set current (Fig. 3*b*), set voltage drop across the specimen (Fig. 3*c*) or at the input (Fig. 3*d*), set power across the specimen (Fig. 3*e*) or at the input (Fig. 3*f*).

The solid, dashed, and dotted lines represent U_{in}, U_{pe}, and U_R, respectively. Similar curves are shown in Fig. 3. The solid, dashed, dotted, and dash-and-dot lines represent P_{in}, P_{pe}, P_R, and $P_{\text{pe}} + P_R$, respectively.

Figures 1–3 correspond to the first radial mode of the TsTBS-3 ceramic 66.4×3.1 mm disk with a pull-up resistor of 11.2 Ω.

The curves represent the "as is" conditions, constant current $I_{pe} = U_R / R = 20$ mV/11.2 Ω = 1.78 mA, constant voltage drop $U_{\text{pe}} = 280$ mV, constant input voltage $U_{\text{in}} = 280$ mV, and constant instantaneous power $p_{00} = 0.04$ W. It can be seen that in the "as is" conditions, the voltage drop U_R reaches its maximum and the voltages U_{in} and U_{pe} reach their minima. To maintain constant current, it is necessary to increase the voltages U_{in} and U_{pe} beyond the resonance. To maintain the constant voltage drop across the piezoelectric element, it is necessary to increase the input voltage, which is accompanied by an increase in the voltage drop across the pull-up resistor at resonance. When the input voltage is set constant, as the resonance is approached, the voltage Upe abruptly decreases and the voltage drop U_R increases. The instantaneous power across the specimen or at the input can be maintained constant by changing the input voltage in a quite complex manner (Fig. 2*e*, *f*).

The instantaneous input power is equal to the sum of instantaneous powers across the piezoelectric element and its pull-up resistor at resonance only. Beyond the resonance, the powers are not equal because the voltages are shifted in phase.

3. Dependence of the Characteristics of the Equivalent Circuit on the Loading Conditions. The radial vibrations of a thin piezoceramic disk were modeled using a Van Dyke equivalent circuit [8, 20, 21] consisting of passive elements $L = 4$ mH, $C = 6.719$ nF, and $C_0 = 25.22$ nF. Thermostable capacitors with mica dielectric and low losses were used. The inductance coil contains two closely spaced, parallel, 0.51-mm-diameter windings, its DC resistance being 6.7 Ω. These passive elements were selected so that their magnitudes and characteristic frequencies were similar to the respective characteristics of the real disk. The equivalent circuit is connected to an advanced Mason two-port network [1, 8, 12, 18, 24] instead of the piezoelectric element.

Figure 4 illustrates the results of modeling for a pull-up resistor of 11.2 Ω. The curves represent voltage drops (first column), input admittance (second column), instantaneous power of the piezoelectric element (third column), and angles of the

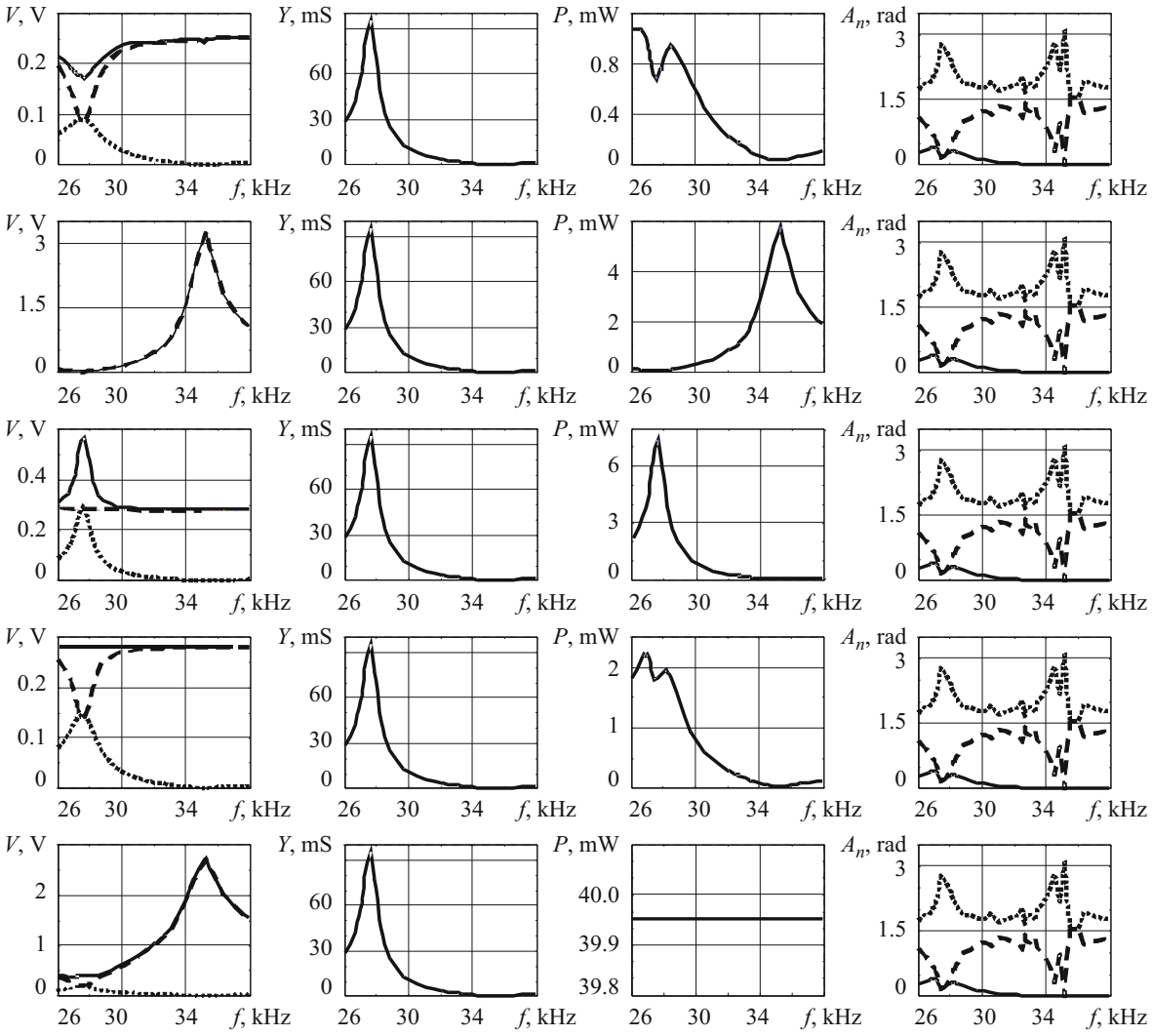

Fig. 4

characteristic triangle (fourth column). The curves represent the "as is" conditions (first row), constant current $I_{eq} = U_R / R = 20$ mV/11.2 Ω = 1.78 mA (second row), constant voltage drop $U_{\text{pe}} = 280$ mV (third row), constant input voltage $U_{\text{in}} = 280$ mV (fourth row), and constant instantaneous power $p_{00} = 0.04$ W. The frequency responses for set current, voltages, and power were plotted by formulas (6) where U_{pe} was replaced by U_{eq}.

The dashed, solid, and dotted lines represent U_{eq}, U_{in}, and U_R. The admittances were calculated by formula (1). The angle α (dotted line) is formed by the sides U_{eq} and U_R of the triangle. It characterizes the phase shift between the current through and the voltage drop across the circuit. The angle β (discontinuous curves) is formed by the sides U_{in} and U_R and characterizes the phase shift between the output voltage and the consumed current. The angle γ (solid lines) is formed by the sides U_{in} and U_{eq}, i.e., it is the phase shift between the output voltage of the generator and the voltage drop across the equivalent circuit.

The curves in Fig. 4 are similar to those of the real disk (Figs. 1–3). When the current (voltage) is set constant, the voltage drop at resonance is lower (higher) than beyond resonance. When the current (voltage) is set constant, the instantaneous power at resonance is lower (higher) than beyond the resonance. At antiresonance, the instantaneous power increases if the current is set constant and decreases if the voltage is set constant. This result somewhat explains the graphs in [27]. The admittance and phase shifts between the sides of the characteristic triangle do not depend on the electric loading conditions; the ratio among U_{eq}, U_{in}, and U_R remain in the linear approximation. The voltages U_{eq}, U_{in}, U_R and their products which are proportional to the instantaneous powers (5) are strongly dependent on the loading conditions.

When the current is set constant, the frequency response of the instantaneous power of the resonator coincides with the frequency responses of the input voltage and impedance. When the voltage is set constant, the frequency response of the instantaneous power coincides with the frequency responses of the current and admittance.

It should be noted that the chosen voltage, current, and power are arbitrary. Therefore, the obtained results can only be used to track tendencies and cannot contain quantitative information. Nevertheless, the figures indicate how the voltages should be changed to provide the required loading conditions.

In addition to the frequency responses of voltage drops, admittances, powers, and phase angles, the voltages U_{pe} (U_{eq}), U_{in}, and U_R measured with an advanced Mason two-port network can be used to also plot frequency responses for current, conductance, susceptance, and instantaneous power.

Conclusions. The oscillatory characteristics of a thin piezoceramic disk near its first radial resonance have been experimentally studied "as are." The behavior of the Van Dyke equivalent circuit consisting of passive *R*-, *C*-, *L*-elements has been studied as well. Based on the experimental data, the frequency responses of voltage drops, admittances, phase shifts, and instantaneous powers for several electric loading conditions have been plotted.

The following conclusions can be drawn.

1. The behavior of piezoelectric transducers strongly depends on the electric loading conditions and differs for (i) set voltage drops across the piezoelectric element or at the input, (ii) set current, (iii) constant input power or instantaneous power of the piezoelectric element.

2. It was established that the voltage drops, input power, and piezoelement power strongly depend on the loading conditions, whereas the admittance, impedance, and phase shifts between the components of admittance do not depend on them. If the current is set constant, the instantaneous power decreases as the resonance is approached and increases as the antiresonance is approached. If the voltage is set constant, the instantaneous power increases as the resonance is approached and decreases as the antiresonance is approached.

3. The impossibility of experimentally studying the vibrations of piezoelectric elements without pull-up resistors [3, 8, 11, 24] results in strong dependence of the phase shifts in the characteristic triangle on these resistors. However, at the resonant and antiresonant frequencies at which the phase shifts between the voltage drop and the current in the piezoelectric element are zero, the effect of the pull-up resistors can be neglected.

4. Modeling piezoelectric elements by *R*-, *C*-, and *L*-elements makes it possible to study their influence on the resonant/antiresonant frequencies and other parameters.

5. Similar results were obtained in studying the influence of the loading conditions on the electroelastic vibrations of thin narrow rods, rectangular plates, circular and cylindrical rings, short and long cylindrical shells, etc. In all cases, it appeared that admittance, impedance, and phase angles do not depend on the loading conditions. These conditions strongly affect only voltage drops, currents in the piezoelectric element, and powers. At harmonics, the pattern is more complex because of the interelectrode capacitance. This problem, however, should be studied separately.

REFERENCES

1. O. Bezverkhii, L. Zinchuk, and V. Karlash, „Effect of the mode of electric loading and direct current or voltage on the vibrations of piezoelectric vibrators," *Fiz.-Mekh. Model. Inform. Tekhnol.*, **18**, 9–20 (2013).
2. O. Bezverkhii, L. Zinchuk, and V. Karlash, "Admittance and instantaneous power of piezoceramic resonators undergoing forced vibrations," *Fiz.-Mekh. Model. Inform. Tekhnol.*, **20**, 27–35 (2014).
3. I. A. Glozman, *Piezoceramics* [in Russian], Energiya, Moscow (1972).
4. GOST 12370-72. *Piezoceramic Materials*, *Testing Methods* [in Russian], Izd. Standartov, Moscow (1973).
5. I. P. Zherebtsov, *Radio Engineering* [in Russian], Svyaz'–Sov. Radio, Moscow (1965).
6. A. M. Kalashnikov and Ya. V. Stepuk, *Basics of Radio Engineering and Radar Ranging* [in Russian], Voenizdat, Moscow (1962).
7. V. L. Karlash, "Energy dissipation during vibrations of thin circular piezoceramic plates," *Int. Appl. Mech.*, **20**, No. 5, 460–464 (1984).
8. V. L. Karlash, "Methods for determining the coupling coefficients for and energy loss in piezoceramic vibrators," *Akust. Visn.*, **15**, No. 4, 24–38 (2012).

9. H. W. Katz (ed.), *Solid State Magnetic and Dielectric Devices*, Wiley, New York (1959).
10. N. A. Shul'ga and A. M. Bolkisev, *Vibrations of Piezoelectric Bodies* [in Russian], Naukova Dumka, Kyiv (1990).
11. M. O. Shul'ga and V. L. Karlash, *Resonant Electromechanical Vibrations of Piezoelectric Plates* [in Ukrainian], Naukova Dumka, Kyiv (2008).
12. M. O. Shulga and V. L. Karlash, "Measuring the admittance of piezoceramic elements in Mason's quadripole circuit and its modifications," in: *Abstracts 4th Int. Sci.-Tech. Conf. on Sensors*, *Devices*, *and Systems*, Cherkasy–Gurzuf (2008), pp. 54–56.
13. M. O. Shul'ga and V. L. Karlash, "Amplitude–phase characteristics of radial vibrations of a thin piezoceramic disk at resonances," *Dop. NAN Ukrainy*, No. 9, 80–86 (2013).
14. B. Jaffe, W. R. Cook, Jr, and H. Jaffe, *Piezoelectric Ceramics*, Academic Press, London and New York (1971).
15. R. Holland, "Representation of dielectric, elastic and piezoelectric losses by complex coefficients," *IEEE Trans. SU*, **SU-14**, 18–20 (1967).
16. "IRE Standards on Piezoelectric Crystals: Measurements of Piezoelectric Ceramics. 1961," *Proc. IRE*, **49**, 1161–1169 (1961).
17. V. L. Karlash, "Resonant electromechanical vibrations of piezoelectric plates," *Int. Appl. Mech.*, **41**, No. 7, 709–747 (2005).
18. V. L. Karlash, "Particularities of amplitude–frequency characteristics of admittance of thin piezoceramic half-disk," *Int. Appl. Mech.*, **45**, No. 10, 647–653 (2009).
19. V. L. Karlash, "Forced electromechanical vibrations of rectangular piezoceramic bars with sectionalized electrodes," *Int. Appl. Mech.*, **49**, No. 3, 360–368 (2013).
20. V. L. Karlash, "Energy losses in piezoceramic resonators and its influence on vibrations' characteristics," *Electronics and Communication*, **19**, No. 2 (79), 82–94 (2014).
21. V. L. Karlash, "Modelling of energy-loss piezoceramic resonators by electric equivalent networks with passive elements," *Math. Model. Comput.*, **1**, No. 2, 163–177 (2014).
22. A. V. Mezheritsky, "Elastic, dielectric and piezoelectric losses in piezoceramics; how it works all together," *IEEE Trans. UFFC*, **51**, No. 6, 695–797 (2004).
23. E. C. Munk, "The equivalent electrical circuit for radial modes of a piezoelectric ceramic disk with concentric electrodes," *Phillips Res. Rep.*, **20**, 170–189 (1965).
24. N. A. Shul'ga and V. L. Karlash, "Measuring the amplitudes and phases of vibrations of piezoceramic structural elements," *Int. Appl. Mech.*, **51**, No. 3, 350–359 (2015).
25. K. Uchino, J. H. Zheng, Y. H. Chen, et al., "Loss mechanisms and high power piezoelectrics," *J. Mat. Sci.*, **41**, 217–228 (2006).
26. K. Uchino, Yu. Zhuang, and S. O. Ural, "Loss detertmination methodology for a piezoelectric ceramic: new phenomenological theory and experimental proposals," *J. Adv. Dielectric.*, **1**, No. 1, 17–31 (2011).
27. S. O. Ural, S. Tuncdemir, Yu. Zhuang, and K. Uchino, "Development of a high power piezoelectric. Characterization system and its application for resonance/antiresonance mode characterization," *Jpn. J. Appl. Phys.*, **48**, 056509 (2009).